Experimental study on the motion response of an integrated floating desalination plant and offshore wind turbine on a non-ship platform

Islam Amin[1,2], Saishuai Dai[2], Sandy Day[2], Mohamed E.A. Ali[3], Ahmed Balah [4], Hosam Shawky[3], Selda Oterkus[2], Erkan Oterkus[2*]

[1] *Department of Naval Architecture and Marine Engineering, Port Said University, Port Said, Egypt*
[2] *Department of Naval Architecture, Ocean and Marine Engineering, University of Strathclyde, Glasgow, UK;*
[3] *Egypt Desalination Research Center of Excellence (EDRC) and Hydrogeochemistry Department, Desert Research Centre, Cairo, Egypt;*
[4] *Irrigation and Hydraulics Department, Ain Shams University, Egypt;*
**Corresponding author: erkan.oterkus@strath.ac.uk; Tel.: +44-141-548-3876*

Abstract

An on-grid floating desalination plant (FDP), powered by conventional fossil fuel, was recently proposed to support freshwater demands in some remote coastal cities that have electricity grid networks. The aim of this study is to investigate feasibility of integrating a wind turbine into the same FDP platform to be suitable for off-grid services with sustainable clean energy resources. The new proposed concept is a fully self-contained mobile system powered by wind. Using a 1:100 scale model of the proposed concept, an experimental study was performed to investigate the floater's motion behavior in Egypt. According to historical sea statistical data for Red Sea in Egypt and taking combined dynamic responses of turbine and floating platform into consideration, frequency and time history dynamic analyses have been done. Furthermore, the possibility of using five different wind turbines in the same FDP platform was studied for upgrading purposes. Results show that the proposed FDP concept has capability to support all tested turbines and to operate safely in Egyptian environmental conditions. Based on the FDP concept with and without turbine comparisons, there are minor motion changes in heave responses, while pitch and surge responses show major changes in time history analyses due to turbine operation.

Keywords: Offshore wind turbine; integrated offshore systems; non-ship floater; seawater desalination; motion response of offshore structure.

1. Introduction

As populations overwhelmingly grow in urban centers in Egypt, demand continues to escalate on current natural water sources in terms of quantity and quality. The small coastal communities, which are far from national water and electricity network grids, face more social and economic challenges, and are facing freshwater shortage crisis. Nonconventional water resources and renewable power can play important roles in the sustainable development of those areas. Desalination has high potential to provide freshwater if combined with renewable energy resources, eliminating the energy-intensive, environment impacts and providing an off-grid power option. The Egyptian government has launched many land-based desalination plants powered by fossil fuel along the Mediterranean and Red Sea coastlines to overcome the main cities' freshwater shortages. Nevertheless, the small remote communities are still far from development. Based on comparisons between different desalination technologies and the ways to power those technologies in the Red Sea region, reverse osmosis (RO) powered by wind energy was determined to be the most cost-effective system (Al-Jabr & Ben-Mansour 2018). Therefore, motivated by social and economic perspectives, a new concept of a wind turbine-powered floating desalination plant was proposed as an innovative solution for small coastal communities.

The novel proposed concept is considered an integration between offshore wind and floating desalination technologies in one offshore platform. With the global interest in the field of renewable energy, floating wind turbine foundations were studied through many numerical and experimental investigations, especially the cylindrical foundation shapes. Chenyu et al. (2018) conducted a comparative analysis of numerical and experimental approaches of a floating wind turbine supported by a spar foundation. The importance of this study is because the floating platform design has a great impact on the motion behavior of the overall floating system. For example, the floating wind turbine's power generation is highly dependent on its motion stability during operation. To minimize the motion effects, Yan et al. (2019) proposed a new concept motion stabilizer connected to the floating wind turbine foundation. In another study, Zhang et al. (2018) tested the dynamic responses of three floating vertical wind turbine models under wind excitations in a water tank. Although the experimental studies are costly and require lengthy preparations, they significantly contribute to the investigation of the complex dynamic responses, which are sometimes difficult to address and manage through numerical methods. A three-bladed vertical turbine model with a geometric scale of 1:100 was used and fixed onto three floating platforms

inspired by offshore oil rigs and floating wind turbine prototypes (Zhang et al. 2018). Guo et al. (2018) studied the dynamic responses of a floating platform support tidal turbine. A 1:100 scaled model of a barge type floater along with a 1:100 scaled model of a NREL 5-MW wind turbine was tested under regular waves (Kumar and Selvar 2013). Similarly, Liu et al. (2017) numerically simulated a motion study of a 5-MW floating vertical axis wind turbine and a cylinder spar-type floating foundation with heave plates. The results showed that the aerodynamic forces have minimal influence on the heave motions of the floating VAWT, but they obviously increase the mean values of surge and pitch motions. The effect of the heave plate on the performance of a semi-submersible cylinder platform was investigated by Antonutti et al. (2014) to improve the heave responses.

With a successful and rapid development of offshore renewable industry, there is an interest in investigating the technological and economic feasibility of combining offshore wind turbines with other industrial applications. Many successful integration applications related to the offshore industry were introduced before. For example, the spar–torus combination, the semi-submersible flap combination, and the oscillating water column array with a wind turbine were studied in detail through numerical and experimental methods (Gaoa et al. 2016). Kamarlouei et al. (2020) introduced a further experimental test of wave energy converters arranged and connected with a floater model. A 1:27 model was tested with and without 12 small wave energy converters. A related research study proposed a novel concept through combining a tension leg platform support floating wind turbine, and a wave energy converter (Ren et al. 2020). Another experimental investigation of a multiple wave converter integrated in a floating breakwater platform was conducted (Howe et al. 2020). Recently, a numerical study discussed a novel floating desalination plant powered by a wind turbine that was proposed to overcome the freshwater problem in remote coastal areas (Amin et al. 2020). Referring to the previous concepts, integrating different applications is a new revolution in the offshore marine industry that could extend its impact on desalination powered by marine renewable energy.

In principle, the floating desalination plants (FDPs) consist of a floating marine base, desalination unit, and power driver. Regarding the foundation shape, the most common FDP concept shape is a ship-shaped configuration, which is designed to produce freshwater and transfer it to the shore directly or a FPSO concept that has the ability to store the desalinated water. A FDP approach was proposed earlier to serve remote islands due to the difficulties of connecting to water grids (Lampe et al. 1979). A ship-shaped mobile desalination vessel was also introduced to supply freshwater to arid coastal communities in another study (Johnson and Clelland 1969). In addition, the FDP concept is used to face high seasonal demand in some coastal areas. For example, Saudi Arabia launched desalination barges to serve some coastal cities in the Red Sea (Proskynitopoulou and Katsoyiannis 2018). With respect to the powering method, a desalination vessel powered by liquefied natural gas was proposed to serve the western Mediterranean coastal cities (Chouski 2002 & 2004). Another desalination ship powered by diesel generation serviced the Emirates and supported three coastal cities on the Arab Gulf coastline (Fadel 1983). In different research works, the principle of using a nuclear source in powering a desalination ship has been explored as a renewable power source (Vasjukov et al. 1992) and (Al-Othmana et al. 2018). In another unconventional concept powered by renewable energy, the Ydriada MUP small floating desalination pilot station was developed and placed in front of one of the Greek islands. The plant was powered by a small wind turbine and had a semi-submersible platform. The pilot station was directly connected to shore with pipe and did not have a storage capacity.

The ship-shaped FPSO concept has several disadvantages, such as complexity in operation due to its unsymmetrical shape, less longitudinal strength due to a large length–beam ratio, insufficient transverse stability in beam wave direction, and the limitations of overturn moment that prevents support of the wind turbines. Therefore, an FDP having a ship-shaped FPSO may not be a good choice in many unusual applications, such as integrated seawater desalination and offshore power generation. For this reason, the desalination industry needs a new unconventional configuration capable of overcoming such disadvantages, such as a cylindrical FPSO concept. Experimental investigation on a non-ship-shaped FPSO was performed to study the vessel motion responses, namely heave and pitch motions under regular waves (Baghernezhad et al. 2017). Based on motion performance, a comparison between the two concepts was conducted that referred to stability, sea keeping, mooring, and riser system loads (Amin et al. 2020). The study concluded that a cylindrical FPSO has better motion characteristics than a ship-shaped concept. In the present study, a novel floating desalination plant and wind turbine integrated into a non-ship platform was proposed and designed for a particular location in Egypt. Since the developed concept is not a conventional unit, the motion response was investigated experimentally to understand the hydrodynamics behavior, which is important for the safety, performance, and operation of such a new hybrid concept. Experimental tests for different loading conditions and wave heights over a range of wave frequencies were performed in a wave tank. Moreover, this study offers a simple approach for simulating the wind turbine aerodynamic loads using an electric ducted fan attached with pulse control system in order to control the thrust force for the desired specific turbine model. Finally, the present results can provide clear explanations for the new concept's performance tested with different turbine models, which will help to implement it into the industry.

2. Proposed FDP concept

The Red Sea region has a high potential to attract Egyptian residents outside the crowded delta of Egypt. There are generally only scattered populations in these areas without water or electricity grids. Development of these regions begins by offering power and freshwater for civil and industrial usages. Amin et al. (2020) previously developed an on-grid FDP plant driven by cables connected to the national grid. As many coastal areas are absent from electricity grids, an off-grid FDP plant powered by wind power was proposed in this study. The concept was proposed for the development of small and remote coastal communities with small and medium water demands. Based on the technical reasons discussed by Amin et al. (2020), a cylindrical platform was selected compared with other offshore platform configurations.

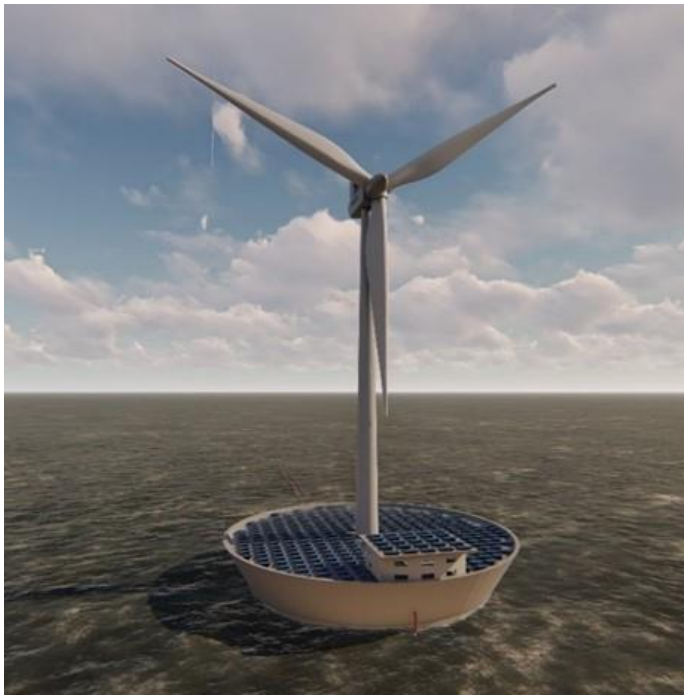

Figure 1: Proposed concept.

The proposed concept was a floating platform supporting a desalination plant, storage tanks, and a wind turbine, as shown in Figure 1. The outer diameter of the main hull was 70 m, and the depth was 32 m. The upper deck diameter was extended to 87.5 m to increase the solar panels' installation area. The heave plate was fitted to the bottom of the hull with a diameter of 87.5 m and a thickness of 2.5 m. A Vestas V112-3MW wind turbine was selected to power the plant. The plant was arranged to place solar panels on the top floor, the RO units and other desalination equipment on the operation deck, and the freshwater storage and ballast tanks in the lower partitions, as shown in Figure 2.

Figure 2: Proposed floating desalination plant concept.

The proposed desalination system is considered a novel system. Most common desalination systems were arranged in parallel configurations, which need large spaces and face losses due to large piping systems. The RO units were designed and simulated by using the Water Application Value Engine (WAVE) software program. Six RO units, each with 2000 m3/day capacity, were designed in a novel circular arrangement to reduce the piping system. The total production of the plant was 10,000 m3/day. The central seawater feeding tank for all RO units was used and connected by feeding pipelines. Each line had its own feeding pump and was equipped with disk filters. The flushing tank and chemical dosing tank were attached to the RO unit and controlled automatically. The proposed naval system is shown in Figure 3.

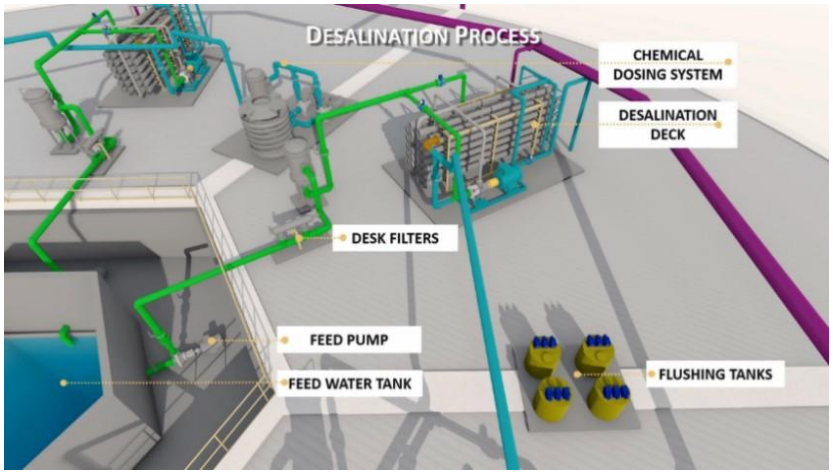

Figure 3: RO desalination system arrangement.

2.1. ***Site location and environmental loads***

The Gulf of Suez and the Red Sea have higher wind energy potential than any other region in Egypt. According to the World Bank's report (2020), Egypt has vast areas along the Gulf of Suez and the Red Sea that have high offshore wind potential for wind energy development. Egypt has 28 GW of potential for offshore fixed wind turbines, while has huge potential expected to be 208 GW for floating wind turbines. Therefore, the offshore wind was selected to be the power source for the proposed FDP desalination plant. Wind density was the critical factor in the selection of the plant site. Based on the annual average wind speed shown in Figure 4 and compared with the International Electrotechnical Commission (IEC) wind class limits, the middle and lower regions of the Gulf of Suez have Class I wind speeds reaching 10 m/s.

Two parameters of the Pierson–Moskowitz (PM) spectra for a range of wave heights and periods were calculated to determine the wave spectrum and wave bands in the Gulf of Suez area as

$$S_{PM}(\omega) = \frac{5}{16}.H_S\,\omega_P^4.\omega^{-5}\,exp\left[-\frac{5}{4}\left(\frac{\omega}{\omega_P}\right)^{-4}\right] \quad (1)$$

where $\omega_P = 2\pi/T_P$ is the angular spectral frequency and

$$\omega = 2\pi f \quad (2)$$

where ω is wave frequency, H_s is the significant wave height and T_P is the wave period.

Based on the recorded wave heights and periods in the Gulf of Suez area (Khalifa etal. 2014), the wave spectrum was calculated for 1-year and 100-year return periods, as shown in Figure 5. According to the spectrum results, the wave bands in the Gulf of Suez area are from 3 to 12.5 s, and the proposed plant should be out of this range to be safe when in operation. Maximum wave height for 100-year return periods is 7.92 m and time period is 8 sec, whereas for 1-year return period it is 5.18 m and time period is 6.5 s.

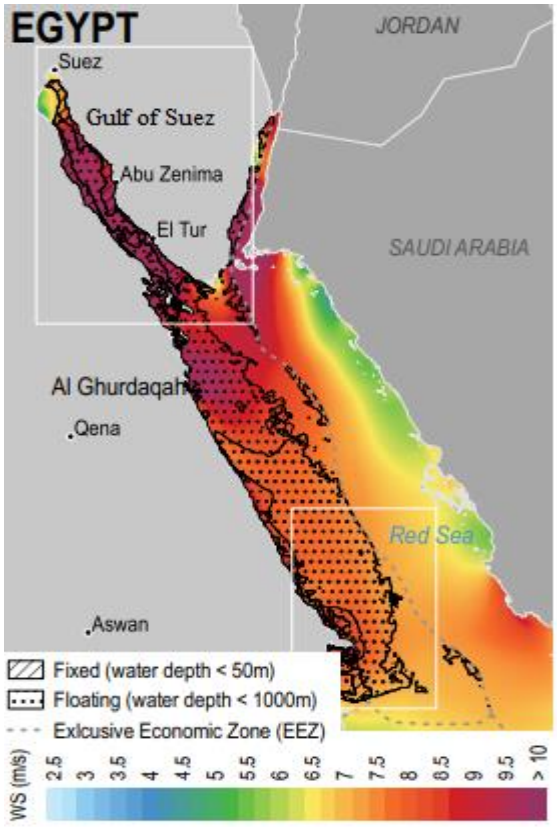

Figure 4: Red Sea offshore wind power potential.

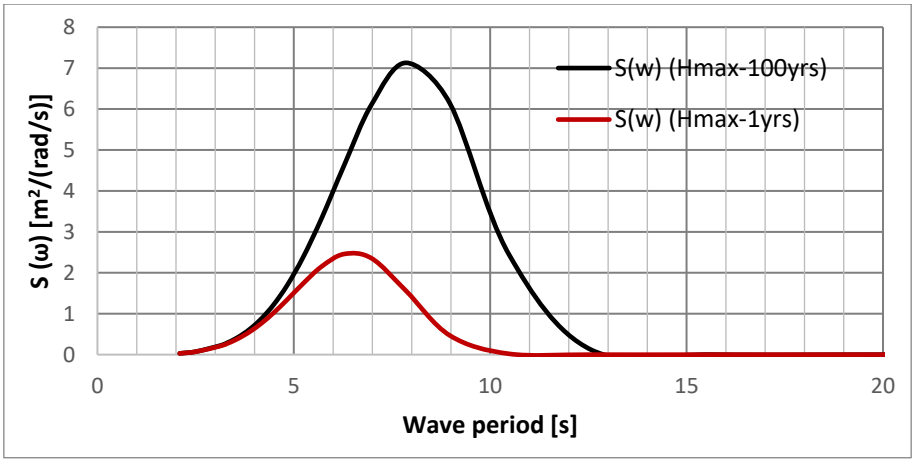

Figure 5. Wave spectrum of Gulf of Suez area.

2.2. ***FDP power consumption***

In previous conceptual designs (Amin et al. 2020), WAVE predicted the RO units' power consumption. The total power consumption to desalinate 10,000 cubic meters of freshwater was estimated at 1591.2 kWh. The power covered all desalination processes, such as filer feed pumps, high-pressure pumps, high-pressure booster pumps, and cleaning and flushing pumps. For marine operation and the accommodation of power loads, the maximum power consumption was estimated to be 1660 kWh for other operating navigation systems, lighting, and control and outfitting devices. The total power needed for all units is 3.2512 MWh (78.029 MW/day). A V112-3MW turbine (72 MW/day) and solar PV arrays on the sun deck (6.12 MW/day) will supply this total power. The plant is equipped with six storage tanks can store 60,000 cubic meters of freshwater to cover any shortage of power production due to environment change or maintenance.

3. Experimental investigation

Experimental tests combining the wind turbine effect and wave environment are important tools for the development of floating wind turbines and other hybrid systems supporting wind turbines, such as FDPs. Although the experimental tests can be costly and time consuming, they can provide accurate performance prediction results. An experimental approach can help the designers ensure the unit's motion performance at the early design stages, especially for novel concepts.

3.1. ***General***

The present experiments were performed at the University of Strathclyde's Kelvin Hydrodynamics Laboratory, using a 1:100 scale model of a cylindrical floating platform supporting a wind turbine. The 1:100 scale factor is selected to reduce reflected wave which is introduced by radiation and diffraction caused by wave structure interaction during the test. The model was moored in the middle of the towing tank, which had a length of 76 m, a width of 4.6 m, and a water depth of 1.91 m. The tank profile and experimental set up are shown in Figure 6.

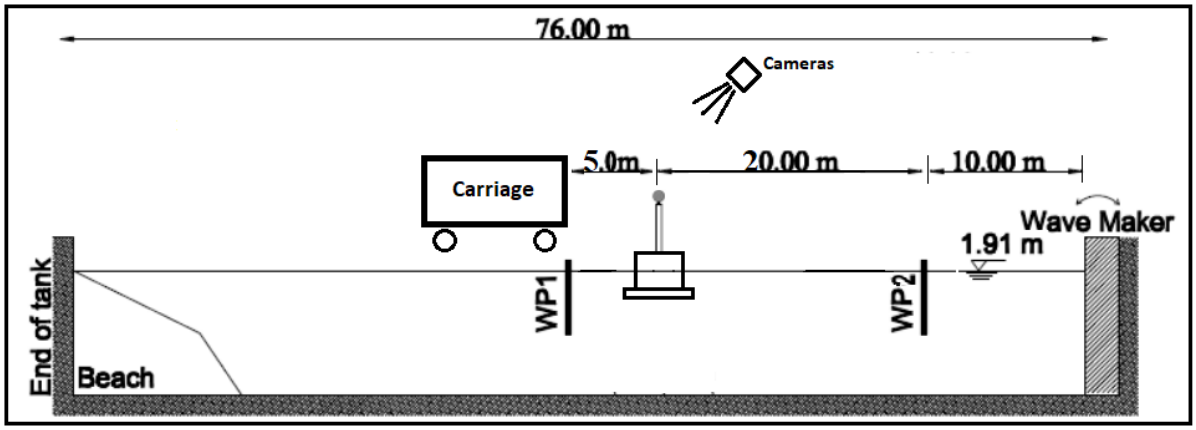

Figure 6: Tank profile and experiment setup.

A wave maker placed at the end of the tank created regular sinusoidal waves. The tank was provided with a carriage that had an electronic control system that could operate and obtain the desired data. Moreover, the tank had absorption facilities to remove the effect of reflected waves. The wave profile was monitored and captured using two probes located 10 m from the wave maker and the ultrasonic wave probe fixed on the carriage.

To monitor the motion of the model, the 6-DOF QUALISYS motion camera system, shown in Figure 7, was used. The model was fitted with four illuminated balls of infrared reflectors attached at the top of the model tower. Four motion capture cameras located above the model adjusted the coordinates of the reflectors in the model space. Then, corrected reflector coordinates to the platform's vertical center of gravity (VCG) at 13.89 cm (model scale) defined the test origin. The model motion was detected with a body-fixed coordinate system, and three motions were calculated and outputted in real time through Spike2 V9.06 data converter.

Four elastic mooring lines moored the model from four corners to maintain the model position during the test. The electrical cables that fed the fan with power and control were connected directly to avoid installing batteries on the model, as shown in Figure 7.

Figure 7: Qualisys camera system attached in the tank roof and the model moored at tank centre in front of carriage.

3.2. ***Model description***

The model hull was constructed based on a full-scale design of an on-grid floating desalination plant, which was introduced by Amin et al. (2020). Amin's plant was modified in this study to an off-grid mode by adding a 3-MW wind turbine at the platform center. Therefore, the current model was equipped with a tower and a fan generating thrust force scaled from the thrust generated from the full-scale turbine. The model had an outer diameter of 0.7 m and a total depth of 0.32 m. The model upper deck had a diameter of 0.875 m, while the heave plate, which was fitted to the bottom of the model, had a diameter of 0.875 m and a thickness of 0.025 m. The cylindrical model was manufactured at the technical workshop of the Kelvin Hydrodynamics Laboratory at the University of Strathclyde in the United Kingdom. The model was built from foam and fiberglass, while wood was used for the upper deck, lower bottom, and heave plate. The turbine tower was made of carbon fiber, and the flange between the fan and the tower was made from plastic. The model is shown in Figure 8.

Table 1. Main design parameters of the proposed FDP concept.

Parameters	Full scale	Scaled (λ=1/100)	Froude Scaling Law
Upper deck diameter [m]	87.5	0.875	λ
Main platform diameter [m]	70	0.7	λ
Heave plate diameter [m]	87.5	0.875	λ
Platform depth [m]	32	0.32	λ
Turbine tower height [m]	86	0.86	λ
Draft [m]	14.4	0.144	λ
Platform displacement [ton]	62680	0.06115	λ^3
VCG [m]	13.89	0.1389	λ
Max turbine load [N]	695000	0.695	λ^3
Wave frequency [Hz]	0.3 to 1.4	0.03 to 0.14	$\lambda^{-0.5}$

The plant has three load-case conditions; namely, lightship, ballast, and full-load conditions were described in detail in a previous experimental study (Amin et al. 2020). The turbine was switched off during the transportation mode (lightship condition). In addition, due to the full storage capacity of the storage tanks, the turbine was switched off in the full-load case. The turbine operating condition was the ballast condition, on which the present study focused to investigate the motion responses. The operating conditions between the ballast case and the full-load case will need more investigation in future work.

The Sesam DVN-GL software was used to design the plant, weight distribution and calculate the VCG and moment. Swing test was used to achieve the target VCG, moment of inertia and radius of gyration as shown in Table 2. The ballasting trial succeed to reach to 0.27% difference in VCG between the model measured value compared to the design target value. While the difference in moment of inertia around Y-axis was about 1.42%.

Table 2. Swing table results for ballast case with fan.

Condition	Ballast condition
mass (kg)	61.1597
Measured VCG (m) from base of the heave plate	0.138524554
Measured Iyy	3.45
Target VCG	0.1389
Target Iyy	3.499788116
Radius of gyration (model scale)	0.239214887
Radius of gyration (Full scale)	23.92148866
Relative difference in VCG	-0.270%
Relative difference in Iyy	-1.42%

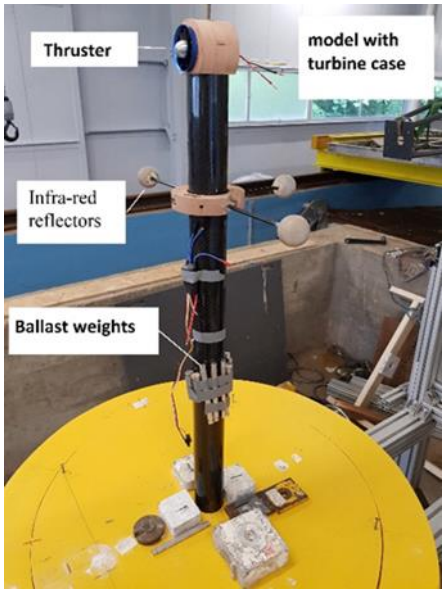

Figure 8: Model with thruster.

3.3. ***Turbine simulation***

Employing a rotating turbine rotor in a wind field generated by a series of fans is one of the most common methods of modelling a floating wind turbine in the laboratory. The Froude scaling law which is usually utilized in such tests may not be matching with the desired aerodynamic loads due to the Reynolds-Number Scaling Effect (Binrong et al. 2020). A blade loading sensing system for model tests of floating wind turbines in the wave tank was proposed by Binrong et al. (2020). Results show that the proposed system successfully captured the turbine blade loads while not smearing other floating wind turbine dynamics. Modern wind turbines have large blade diameters and are lightweight, which include technical challenges for the construction of the scaled rotor and achieve correct weight and structural properties. While using a scaled blade model with high accuracy and precision, wind generation can provide a satisfactory thrust load. However, such method normally requires expensive model construction due to the challenge in the ultra-light blade requirement. Therefore, a simple method such as employing a ducted fan to model the thrust load from the rotor is considered as an attractive solution to generate a predefined value of thrust (Oguz et al. 2018). To simulate the thrust load of the turbine rotor, an electric ducted fan (EDF) was employed. An electric control system is used by the pulse width modulation technique (PWM) via an electric speed controller (ESC) to drive the fan rotation speed. This technique is often used in radio-controlled (RC) hobby aircraft. Prior to testing, the EDF was first calibrated by rigidly connecting it to a single-degree load cell. The calibration was achieved by varying the throttle of the EDF from 0 to 100%, and the corresponding thrust was then recorded. In this way, the power input was found to achieve a desired thrust load. The calibration setup is shown in Figure 9.

The key benefits of the present EDF approach are summarized below.

1. No need for a wind generation system that has higher costs.

2. Saves time to construct another scale model of the turbine rotor and its driver.
3. Experiment is dictated only by the hydrodynamics of the floater, which helps to enlarge the model test scale.
4. The forces generated by an EDF steady wind are not dependent on the model wave directions.

Figure 9: Electric Ducted Fan (EDF).

3.4. ***Steady wind in calm water***

To evaluate the stability performance of the FDP, the pitch list angle of the model was recorded under different steady EDF loads. By simulating steady thrust force cases in calm water without waves, the effect of the aerodynamic loads of the turbine on the FDP model were evaluated. Antonutti et al. (2014) concluded the wind-induced inclination limit (about 6 degrees) to keep the wind turbine operating efficiently. Figures 10 and 11 show the surge and pitch responses of the system when a range of steady EDF thrust loads (from 0 to 3.5 N) were applied. As shown in Figure 10, there is a linear relation between list angles and EDF load values. The linear equation was estimated in order to obtain interpolation values if required in the future. Similarly, the surge stiffness was recorded for different EDF loads, and the linear equation was estimated, as shown in Figure 11. The maximum pitch angle (about 2 degrees) occurred when 3.5 N thrust force was applied.

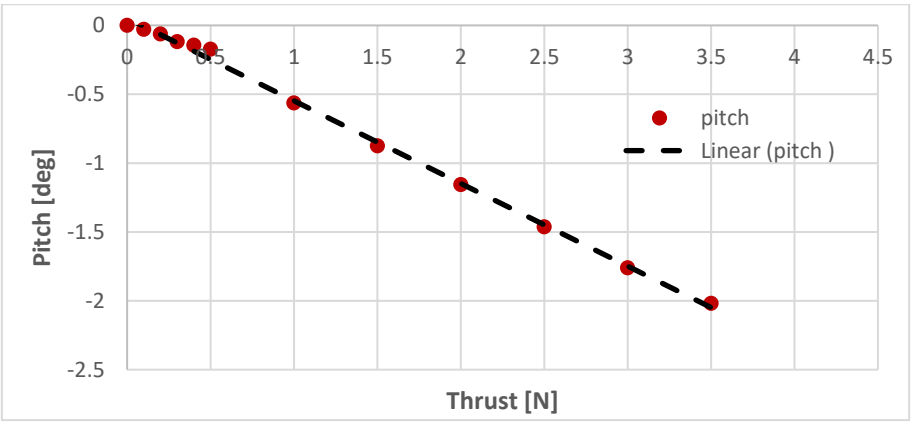

Figure 10: Pitch list angle versus different thrust force.

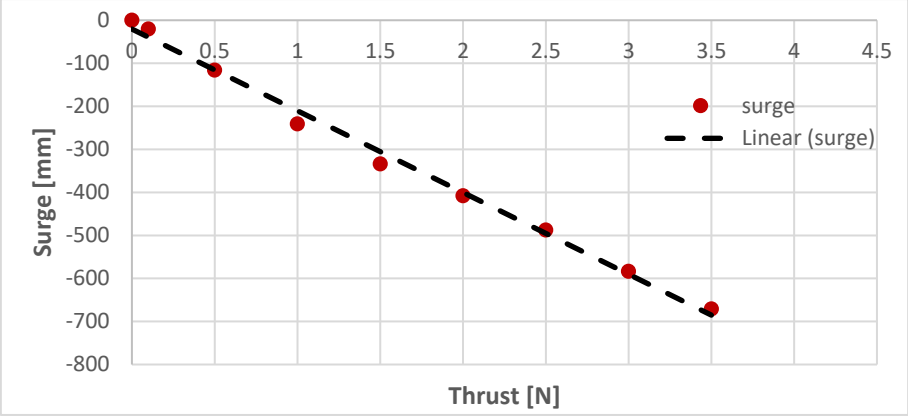

Figure 11: Surge list angle versus different thrust force.

4. Experimental Motion responses

Dynamic responses of floaters in their deployment area have a critical impact on the overall performance of the whole structure system. Understanding the impact of wind turbine loads on the motion behavior of the proposed FDP concept is beneficial to the design of such concepts.

4.1. ***Influence of the turbine operation on the dynamic Performance of FDP model***

The motion responses of the FDP model with and without an operating turbine in surge, heave, and pitch motions were measured in the present experiments. The platform with a turbine means the EDF operates and without means that the EDP switched off. These responses were expressed in terms of RAOs by normalizing with respect to the incident wave amplitude. The heave and pitch RAOs for the FDP models with and without an operated fan are presented in Figures 12(a) and 12(b), respectively.

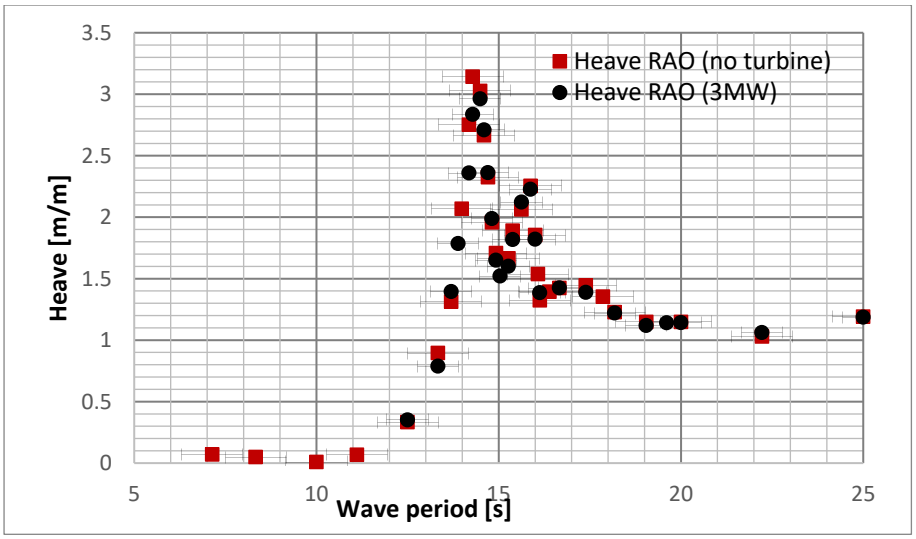

(a)

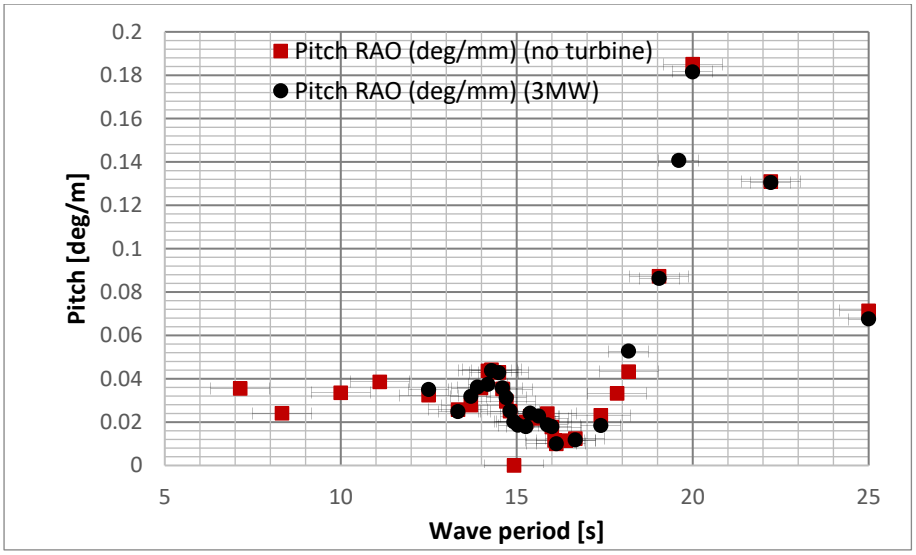

(b)

Figure 12: Comparison of (a) heave RAO and (b) pitch RAO for FDP concept with/without turbine.

The heave RAOs obtained for the FDP concept with and without the 3-MW wind turbines are shown in Figure 12 (a). It is observed from Figure 12(a) that the influence of adding an operated turbine to the FDP model on the motion response is very small. For the FDP without a wind load case, the peak responses of heave motion are equal to 3.14 (m/m) and occurred at a wave period of 14.28 s (0.07 Hz) at full scale. For the proposed FDP concept with a 3-MW turbine, the heave peak is shifted to 14.5 s, and the heave RAO is reduced to 2.96 (m/m). Thus, the heave response is slightly lower when compared to a FDP with a 3-MW turbine case. The pitch motion peak responses accrued at 20 s for both cases.

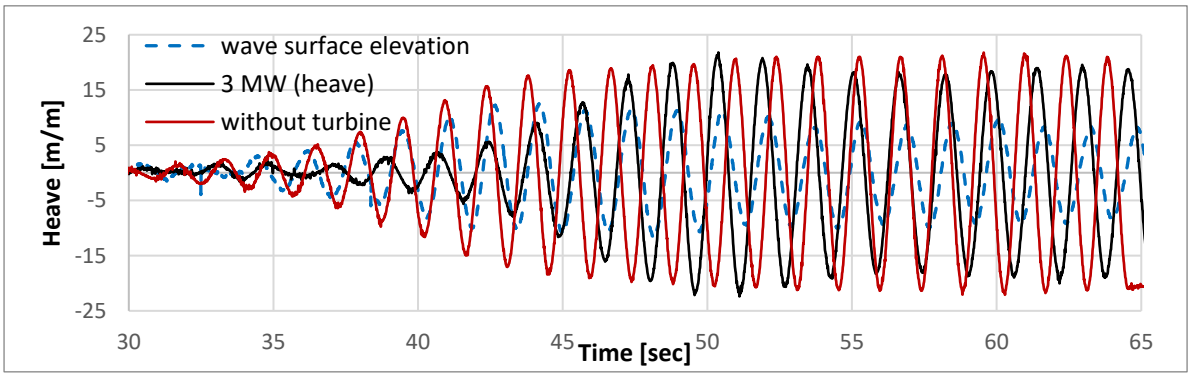

Figure 13: Time history of wave surface elevation and its corresponding heave response

The time series of the heave response of the FDP model with/without turbine at 14.28 s (response peak) and the wave surface elevation inside the tank is shown in Figure 13. It is important to notice that the wave elevations and heave responses for both cases are not in phase motion but are recorded separately in different running cases. The aim of the present comparison is to show the effect of adding EDP loads on the heave motion of the FDP. The heave of the model with a turbine is about 2.94 times the incident wave height at this wave period. The heave RAO of the model was increased to 3.14 times with the addition of a 3-MW turbine near the natural frequency. The surge time history of the FDP model with an operated turbine is shown is Figure 14. When the test was began, it was observed that the model with a turbine moved backwards when the fan started working and significantly oscillated in the x-axis, as shown in the surge motion response in Figure 14. It's noticed that small drift happened when the tank wave arrived to the model, also illustrated in Figure 14. When the EDP loads were equal to the tension in the front elastic mooring lines, the model stopped drifting into new positions. The heave time response history has shown slight decrease in response in the case of the FDP model with a turbine rather than without a turbine. In pitch response motion, it is observed that fluctuation range increased and oscillated around a new equilibrium listing angle, as shown in Figure 15. Furthermore, the pitch motion can be remarkably increased in the case of the FDP model with a wind turbine compared with the FDP without a fan.

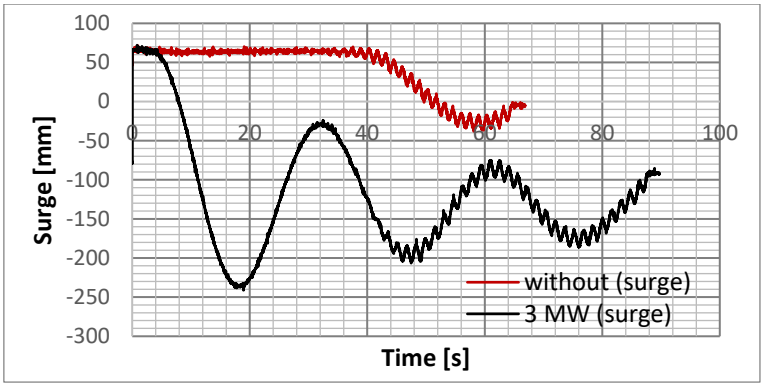

Figure 14: Surge time history for FDP model with/without turbine.

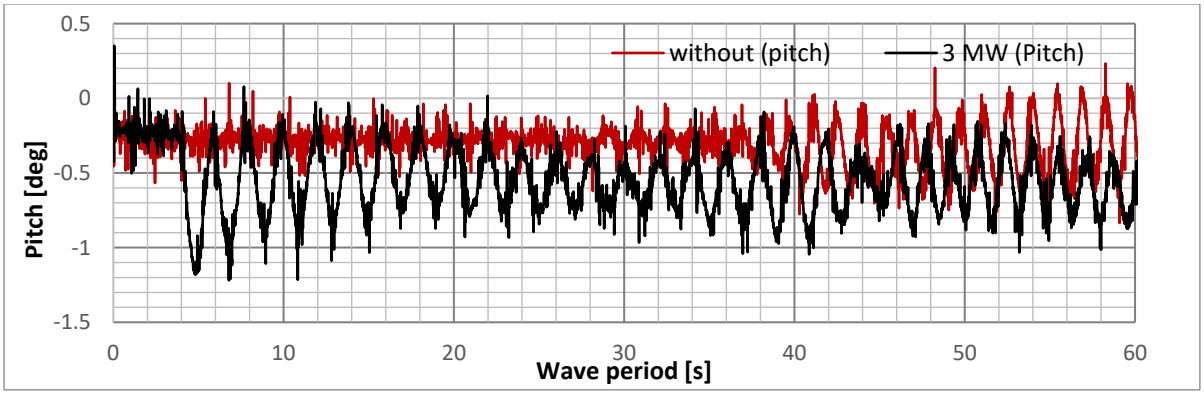

Figure 15: Pitch time history of FDP model with/without turbine.

4.2. Influence of wave steepness on the RAO

To evaluate the effect of change in wave steepness on RAO results of the FDP model with a turbine, two wave heights were considered. The measured heave and pitch RAOs for the two wave steepness values of 0.0053 and 0.0785 are shown in Figures 16 and 17. The selected wave heights were presented with the significant wave height for a 1-year return period (2.15 m for wave period 5.08 s) and a 100-year return period (5.18 m for wave period 6.5 s). In the heave response, it can be observed that the influence of wave steepness is very significant in the natural period of the model. However, for the remaining wave period ranges, there is no significant change in heave RAO results. In pitch responses, the effect of wave steepness on RAO is more evident and remarkable for all wave period ranges rather than in the heave responses. The heave RAO results matched with the results of a previous study presented by Amin et al. (2020) on the effect of wave height on RAOs of the FDP model without a turbine. While the influence of wave steepness for pitch motion on the FDP model with a turbine is more significant for all wave period ranges compared with the FDP model without a turbine. Therefore, it can be concluded that the influence of the wave steepness on the motion responses of the FDP model with a turbine is more significant, especially in pitch responses, and cannot be considered marginal.

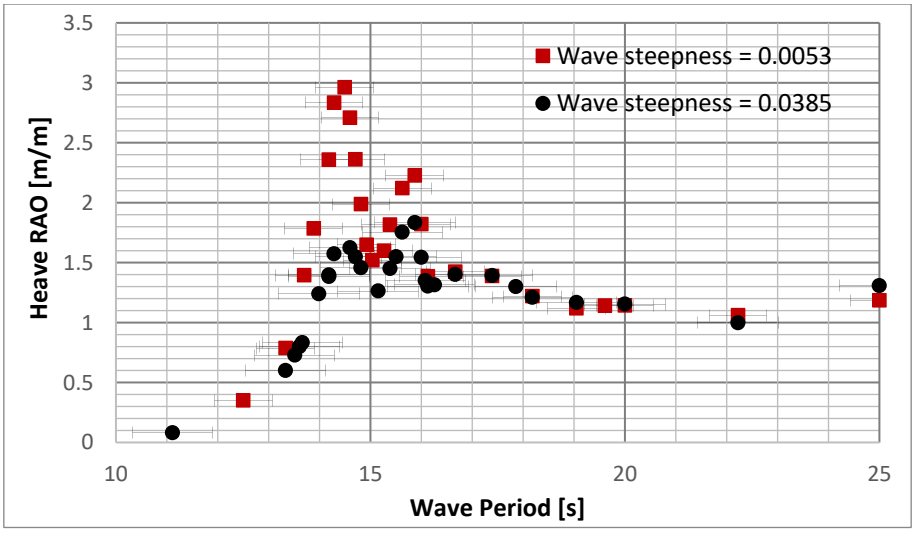

Figure 16: Heave RAO for different wave steepness.

In the natural frequency range, it can be noticed that the heave response has a nonlinear relationship with wave height. The heave responses decrease with the increasing wave height, as shown in Figure 16. While in pitch responses, the responses decrease when the wave height increases near the natural heave frequency and increases when the wave height increases near the natural pitch frequency, as shown in Figure 17.

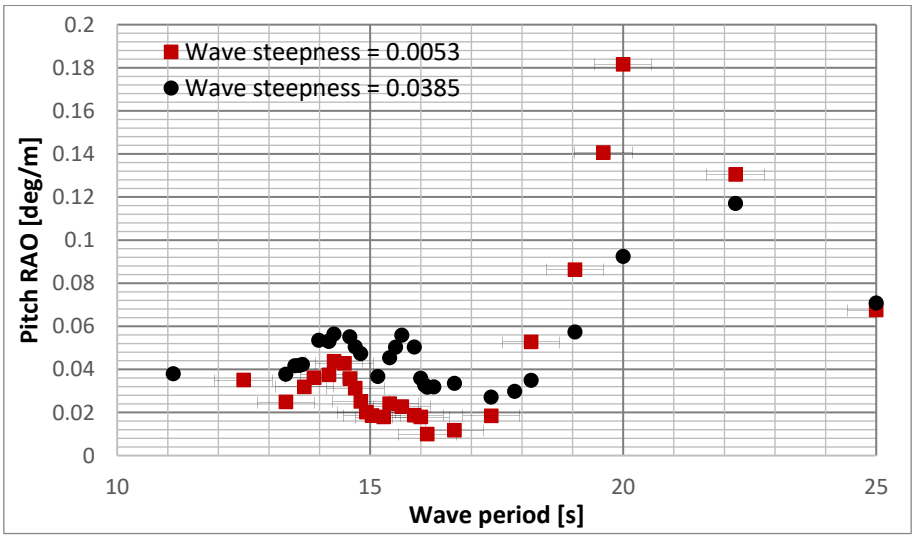

Figure 17: Pitch RAO for different wave steepness.

5. Possibility of use of other turbines

5.1. Turbines specifications

Five viable options were identified in the present study to investigate the possibility of upgrading the turbine capacity. In addition to the 3-MW turbine, which was previously introduced in section 3, the 2-MW Vestas wind turbine, the 5-MW wind turbine devised by the National Renewable Energy Laboratory (NREL), the LEANWIND 8-MW reference turbine (LW), and the 10-MW turbine described by the Technical University of Denmark (DTU) were evaluated experimentally. The turbines' specifications were summarized in Table 3. Since the wind turbine contribution to the total mass property is relatively small compared with the total platform structure and ballast weights (as shown in Table 3), similar total system mass properties can be achieved with the redesign of the ballast. Therefore, the turbine total weight for each case is considered by adjusting the model ballast weight.

Table 3 Turbines specifications summary.

Turbine manufacture	Vestas	Vestas	NREL	LW	DTU
Rating	2 MW	3 MW	5 MW	8 MW	10 MW
Diameter	90	112	126	164	178.3
Hub height	65	86	90	100	110
Rated speed	12	12	11.4	12.5	11.4
Cut-off speed	25	25	25	25	25
Max tower top thrust [kN]	240	695	1619	2743	3242
Scale thrust [N]	0.24	0.695	1.619	2.743	3.242
Rotor weight	36	41	56	90	105
Tower weight	68	70	347	558	605
Nacelle weight	224	230	240	285	446
Total	328	341	643	933	1156
Turbine weight/total system weight [%]	0.52	0.54	1.02	1.48	1.84

Based on the thrust coefficient, which was obtained from turbine manufacture data, thrust force versus wind speed was plotted in Figure 18. The maximum thrust for all turbines was achieved at wind speeds between 10 to 11 m/s, which are suitable to the average wind speed in the Suez Gulf area. The thrust force for each turbine was modelled based on Froude law for each turbine. During the experiments the tower height of 3 MW turbine was kept constant for all turbines (86 cm in model scale). Whereas the maximum turbine top thrust moment was modified and corrected for other four turbines to be equivalent to their tower heights. Total turbine weight is considered by controlling the ballast weight, while the change of hub and tower weights between turbines was assumed to be neglected compared with total plant weight.

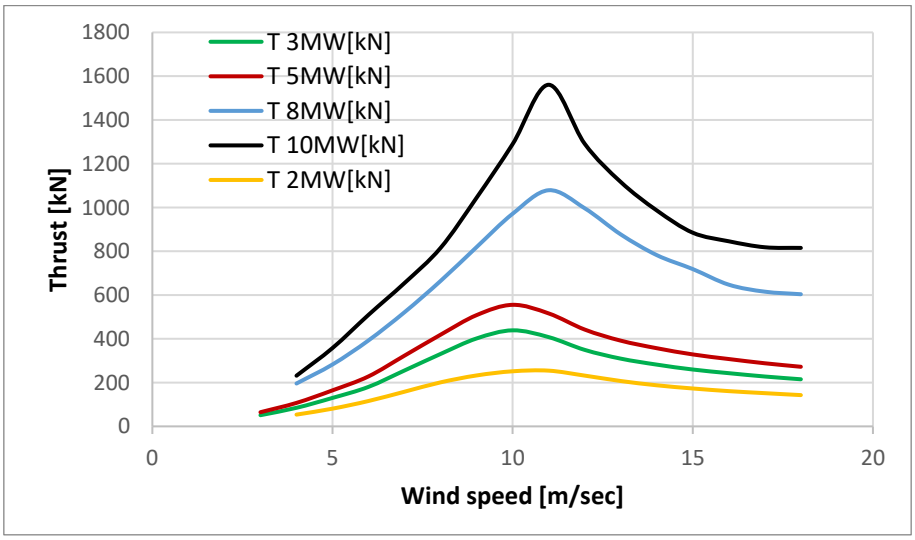

Figure 18: Thrust forces for different wind turbines.

The thrust load from the rotor of each turbine was simulated by EDF to generate a predefined scale value of true turbine thrust. The calculated maximum thrust load and the scaled value are shown in Table 2.

5.2. Motion time history of FDP model with different turbines

The pitch time series of the FDP model with different turbine capacities are presented in Figure 19. It can be observed that the pitch angle increased when the turbine capacity increased. The maximum pitch angle was recorded by the 10-MW turbine at 3.3 degrees, while the lower pitch angle was recorded for the FDP model without a turbine. The dynamic fluctuation range of the 10-MW turbine is the largest compared with the other turbines, while the FDP model without a turbine has the lowest pitch motions

Using the pulse width modulation technique via an electric speed controller, the drive of ducted fan rotation speed can be achievable as described in section 3. Five thrust loads was scaled and calibrated to be equivalent to maximum thrust force for each mentioned turbines.

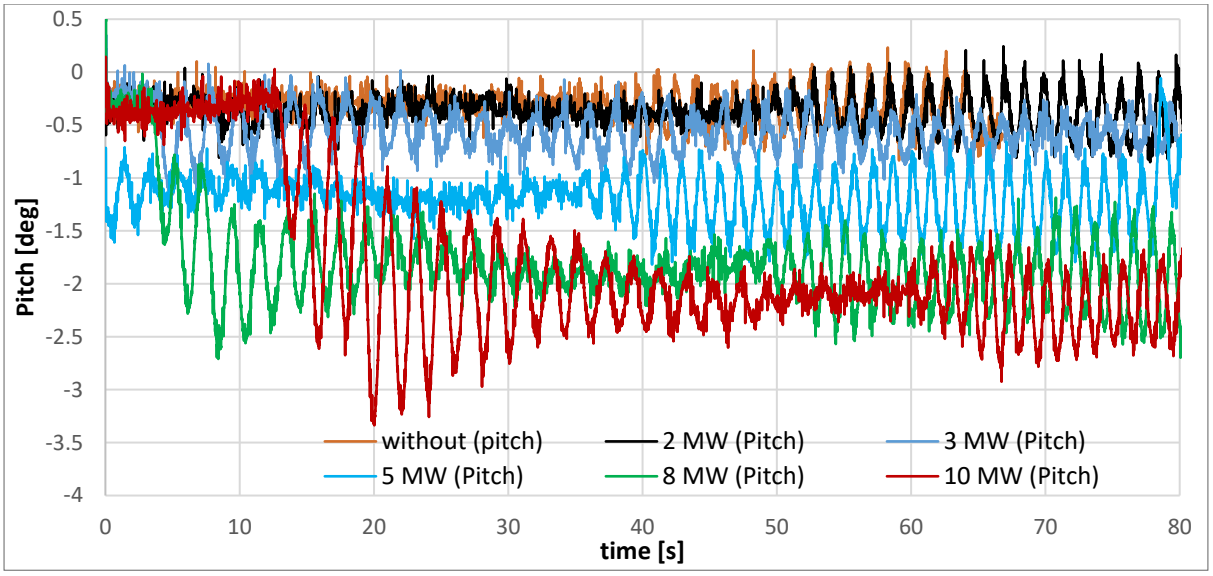

Figure 19: Pitch time history for different turbine capacities.

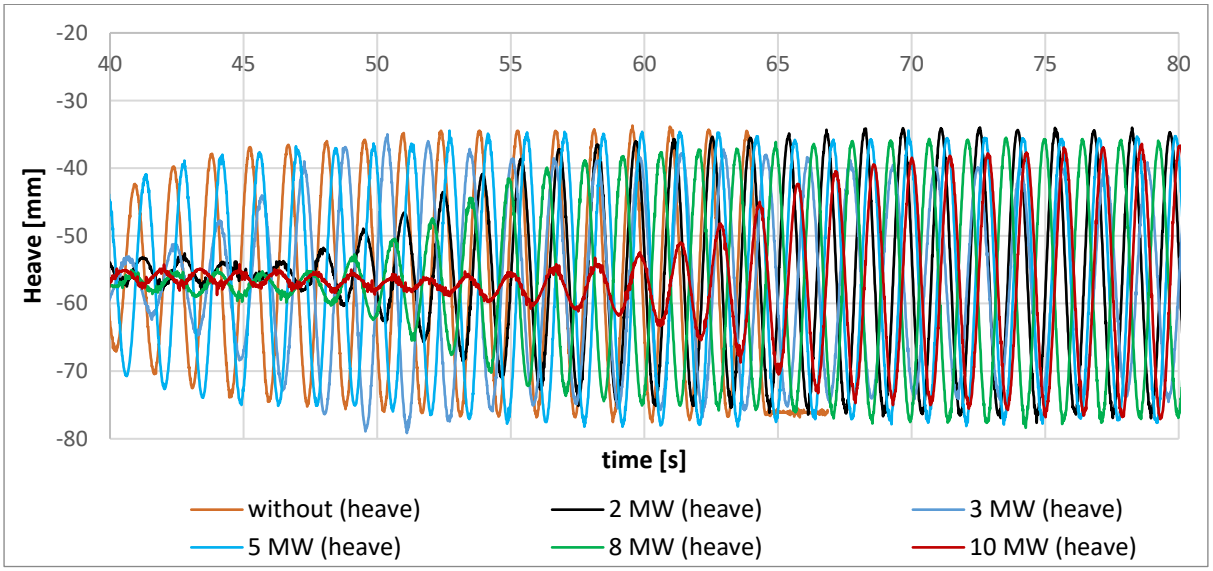

Figure 20: Heave time history for different turbine capacities.

The surge time history is significantly affected by the turbine thrust capacity. It is observed that the change in model position in the x-axis and the surge fluctuation due to an increase of the turbine thrust capacity is shown in Figure 21. In the no turbine case, the surge responses are almost zero, but they begin to increase by increasing turbine thrust. Similar to pitch time history, in the on turbine case, there is no list angle, and the model fluctuated in the narrow-band range. When the turbine was operating, significant changes in the pitch list angle and fluctuation band range were observed. At the heave time history (natural model period), shown in Figure 20, the heave responses were reduced by increasing the turbine thrust force, and this observation cannot be separated from the tension that occurred in the front elastic mooring lines. The influence of the change in model position due to the turbine operation can be observed throughout the surge displacement in Figure 21 for all turbine capacities.

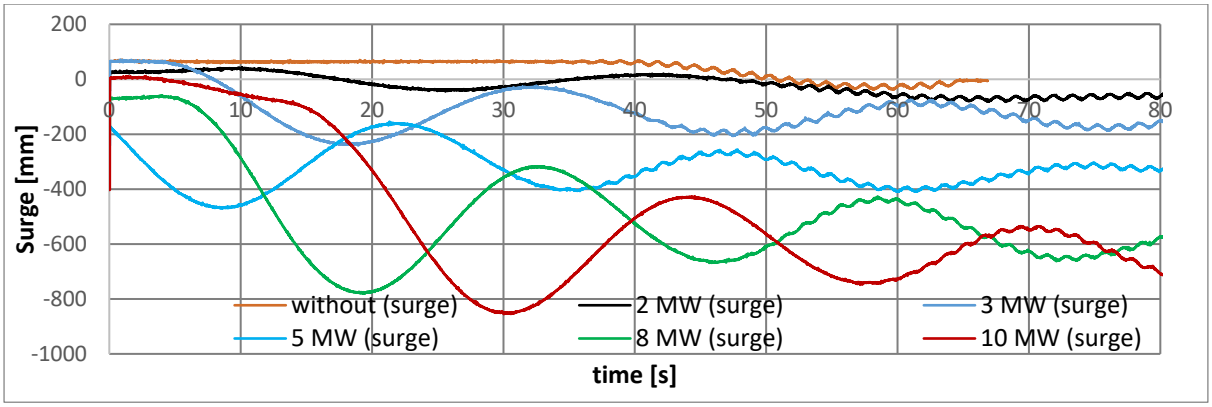

Figure 21: Surge time history for different turbine capacities.

5.3. Comparison of heave and pitch RAOs for FDP model with different turbines

Comparisons of the heave and pitch RAOs were conducted in Figures 22 and 23 to illustrate the possibility of use different turbines in the same platform. The heave RAO is reduced by increasing the turbine capacity due to the additional damping force occurring from the mooring lines, especially at peak range when compared with the no turbine case. The pitch RAO is increased by increasing the turbine force capacity in the model's natural peak and the secondary peak.

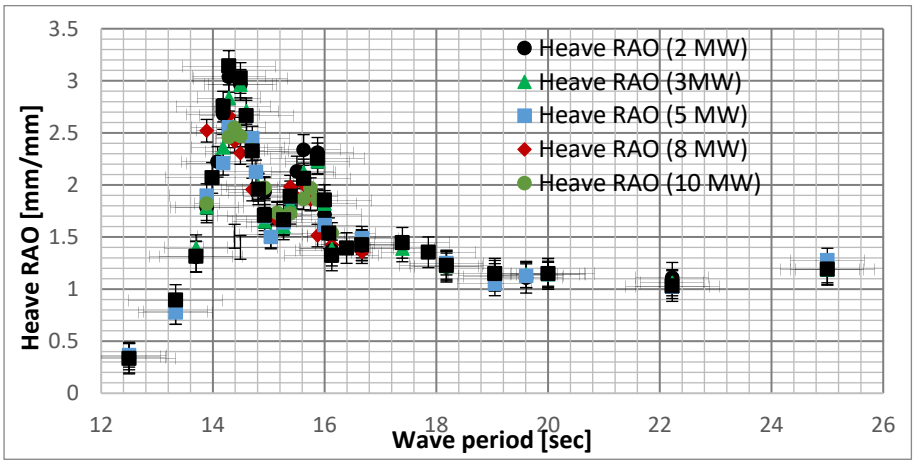

Figure 22: Heave RAO for different turbine capacities.

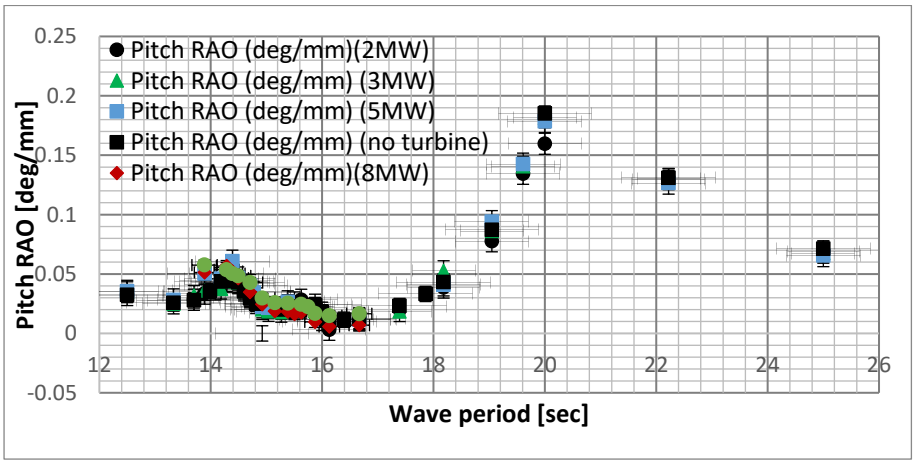

Figure 23: Pitch RAO for different turbine capacities.

5.4. Suitability of proposed concept to Egypt

Generally, the floater motion responses should be suited to the site for which it is designed. In the case of installation of a wind turbine on a floating platform, additional requirements due to the turbine aerodynamic forces and torques are required. The platform's dynamic motion may lead to a change in the displacement angle of the tower during the operation of the turbine. The decline angle should not increase more than 6 degrees to avoid any negative effects on turbine operation and performance (Antonutti et al. 2014). As shown in Figure 19, the maximum dynamic pitch angle occurred for the model supporting the 10-MW turbine at about 3.3 degree. Therefore, all turbines evaluated in this study were under the decline limit of turbine performance. Moreover, the natural period of the platform should be outside of the energy excitation range of the waves to avoid resonance and its dangerous consequences. The natural heave and pitch frequencies for the proposed platform were obtained from the peak responses of heave and pitch RAOs in Figures 22 and 23 at 14.28 s (0.07 Hz) and 20 s (0.05 Hz), respectively. DNV guidelines (2013) recommend that the natural frequency of the floater should not come close to the excitation frequencies arising from the imposed environmental loads. Furthermore, the system's frequency should be away from the operating blade passing frequencies (1P) and 2P/3P frequencies, which are related to two-bladed and three-bladed wind turbines. The wave spectra of the Red Sea zone, floater neutral frequency zone, and the 1P and 3P frequencies for all five turbines, which were provided by the producer, were plotted in the power spectral density diagram in Figure 24. The proposed platform natural frequencies are outside of the wave excitation force of the Red Sea and out of all turbines' operating frequencies.

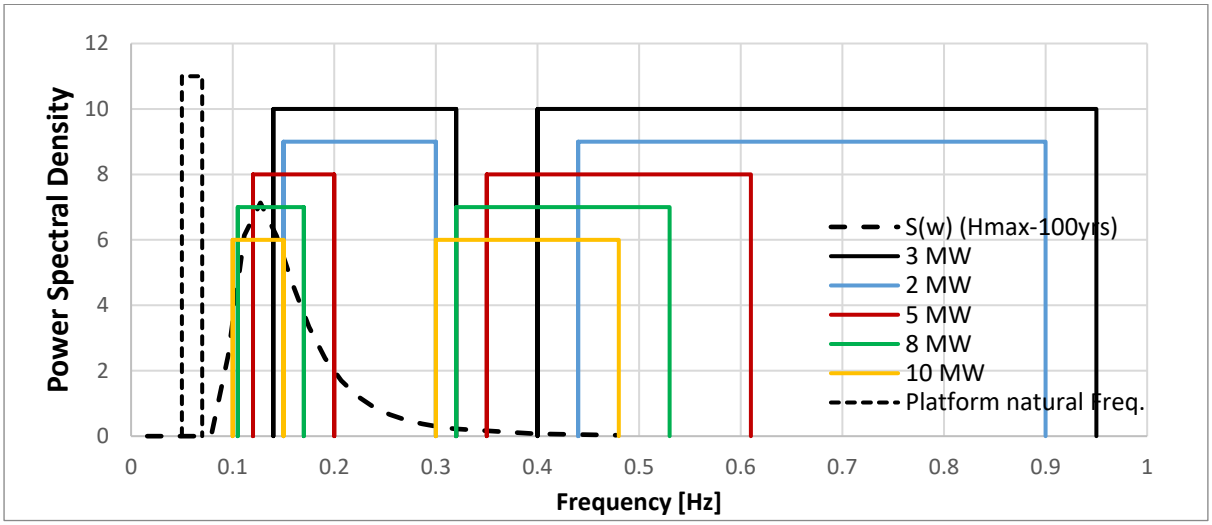

Figure 24: suitability of proposed FDP concept for Red Sea area for different wind turbines.

6. Conclusion

In the present paper, an experimental study on a novel FDP model with a wind turbine was investigated. The dynamic responses of the FDP models with and without a turbine were obtained by experimental tests conducted at Kelvin Hydrodynamics Laboratory of University of Strathclyde in the United Kingdom. The objective of this study is to understand the motion behavior of the FDP with a wind turbine and the possibility of using different wind turbines for the same platform. The results show that the pitch responses have a major impact due to the turbine's operation. The pitch responses and list inclination angle increase when the turbine thrust loads increase or when a larger turbine is installed. Dynamic pitch fluctuation bands increased by increasing the thrust force and should be considered in addition to the static list inclination angle in the stability evaluation. Unlike pitch trends, heave responses were slightly decreased by adding a turbine and increasing the turbine thrust forces. The tension that occurred in the front elastic mooring lines was observed during the test and may be responsible for the heave response reduction. No change in the model's natural period for heave and pitch RAOs due to turbine operation was observed for the all of the turbine forces capacities. It is observed that the pitch RAO and the frequency domain analysis do not reflect the changes that occurred due to adding a turbine to the FDP platform and are not sufficient tools to capture the dynamic behavior of such a coupled platform–turbine system. Nevertheless, the time history analysis is essential for presenting the dynamic fluctuation band with the new list angle in each thrust force. Therefore, development of experimental testing methodologies of floater support wind turbines is needed due to the complex nature of the interaction between the hydrodynamics and aerodynamics loads applied by the

turbine and its foundation floater. The suitability of the proposed concept with different wind turbine capacities was evaluated, and the FDP concept natural frequencies were determined and compared with wave excitation forces in the Red Sea. The experimental results show compatibility between 1P turbine frequency for NREL, LW and DTU turbines (5, 8 and 10 MW respectively), while Vestas turbine 2 and 3 MW are suitable and out of all turbine operation frequencies and wave excitation band in Red Sea deployment area. Based on the model scale results, pilot station is recommended to be considered in further studies.

Acknowledgements

The authors acknowledge the British Council and Science and Technological Development Fund (STDF) for supporting the project NO. 30707 (Mobile Reverse Osmosis Floating Desalination Platform Powered by Hybrid Renewable Energy). The authors acknowledge the University of Strathclyde's Department of Naval Architecture, Ocean and Marine Engineering and Desert Research Centre for the technical expertise and support provided during the period of research. The authors would also like to acknowledge the Kelvin Hydrodynamic Laboratory technician team including Steven Black, Grant Dunning, Bill Wright, Rebecca McEwan for their technical support through the model construction and experiment setup.

References

Al-Jabr, A and Ben-Mansour, R. 2018. Optimum Selection of Renewable Energy Powered Desalination Systems. Proceeding. 2: 612.

Al-Othmana, A., Darwishb, N., Qasima, M., Tawalbehc, M., Darwisha, N. and Hilald, N. 2019. Nuclear desalination: A state-of-the-art review. Desalination. 457: 39–61.

Amin, I., Ali, M., Bayoumi, S., Oterkus, S., Shawky, H. and Oterkus, E. 2020. Conceptual Design and Numerical Analysis of a Novel Floating Desalination Plant Powered by Marine Renewable Energy for Egypt. Journal of marine science and engineering. 8: 95. (doi:10.3390/jmse8020095).

Amin, I., Dai, S., Oterkus, S., Day, D. and Oterkus, E. 2020. Experimental investigation on the motion response of a novel floating desalination plant for Egypt. Ocean Engineering. 210: 107535.

Amin, I., Ali, M., Bayoumi, S., Balah, A., Oterkus, S., Shawky, H. and Oterkus, E. 2021. Numerical Hydrodynamics-Based Design of an Offshore Platform to Support a Desalination Plant and a Wind Turbine in Egypt. Ocean Engineering. 108598.

Antonutti, R., Peyrard, C., Johanning, L., Incecik, A. and Ingram, D. 2014. An investigation of the effects of wind-induced inclination on floating wind turbine dynamics: heave plate excursion. Journal of Ocean Engineering. 91: 208-217.

Baghernezhad, N., Edalat, P. and Etemaddar, M. 2017. Hull Performance Assessment and Comparison of Ship-Shaped and Cylindrical FPSOs with Regards to: Stability, Sea-Keeping, Mooring and Riser Loads in Shallow Water. International Journal of Marine Technology (IJMT). 8: 1-13.

Chenyu, L., Gao, Z. and Moan, T. 2018. Comparative analysis of numerically simulated and experimentally measured motions and sectional forces and moments in a floating wind turbine hull structure subjected to combined wind and wave loads. Engineering Structures. 177: pp 210-233.

Chouski, B. 2002. Aqua TDP/B3DP plants and systems: Floating modular dismountable desalination equipment. Desalination. 153: 349–354.

Chouski, B. Aqua TDP/S3DP plants and systems. 2004. Floating ship-borne modular dismountable seawater desalination plant. Desalination. 165: 369–375.

Design of Floating Wind Turbine Structures, DVN-GL rule, DNV-OS-J103, JUNE 2013.

Fadel, M., Wangnick, K. and Wada, N. 1983. Floating Desalination Plants an Engineering, Operating and Economic Appraisal. Desalin. J. 45: 49–63.

Gaoa, Z., Moan, T., Wan, L. and Michailides, C. 2016. Comparative numerical and experimental study of two combined wind and wave energy concepts. Journal of Ocean Engineering and Science. 1: 36-51.

Guoa, X., Yang, J., Lua, W. and Li, X. 2018. Dynamic responses of a floating tidal turbine with 6-DOF prescribed floater motions. Ocean Engineering. 165: pp 426-437.

Howe, D., Nader, J. and Macfarlane, G. 2020. Experimental investigation of multiple Oscillating Water Column Wave Energy Converters integrated in a floating breakwater: Energy extraction performance. Applied Ocean Research. 102086.

Johnson, K. and Clelland, D. 1967. Mobile and Floating Flash Desalination Plants. Desalination. 2: 170–174.

Kamarlouei, M., Gaspar, J., Calvario, M., Hallak, T., Mendes, M., Thiebaut, F. and Soares, C. 2020. Experimental analysis of wave energy converters concentrically attached on a floating offshore platform. Renewable Energy. 152: 1171-1185.

Khalifa, A., Haggag, S. and Fayed, M. 2014. Fatigue Assessment Analysis of Offshore Structures with Application to an Existing Platform in Suez Gulf, Egypt. World Appl. Sci. J. 30: 1000–1019.
Kumar, G. and Selvar, R. 2013. Experimental investigation of barge floater with moonpool for 5 MW wind turbine. Journal of Information, Knowledge and Research in Mechanical Engineering. 2(2): 488.
Lampe, H., Altmann, T., and Giitjens, H. 1997. PCS—Preussag Conversion System Mobile floating seawater desalination plant. Desalination. 114: 145–151.
Liu, L., Guo, Y., Zhao, H. and Tang, Y. 2017. Motions of a 5 MW floating VAWT evaluated by numerical simulations and model tests. Ocean Engineering. 144: 21-34.
Offshore Wind Technical Potential in the Arab Republic of Egypt. The World Bank, Washington DC 20433, March 2020.
Oguz, E., Clelland, D., Day, A., Incecik, A., López, J., Sánchez, G. and Almeria, G. 2018. Experimental and numerical analysis of a TLP Floating Offshore Wind Turbine. Ocean Engineering. 147: 591-605.
Proskynitopoulou, V. and Katsoyiannis, I. 2018. Review of Recent Desalination Developments for more Efficient Drinking Water Production across the World. New Mater. Compd. Appl. 2: 179–195.
Ren, N., Ma, Z., Shan, B., Ning, D. and Ou, J. 2020. Experimental and numerical study of dynamic responses of a new combined TLP type floating wind turbine and a wave energy converter under operational conditions. Renewable Energy. 151: 966-974.
Vasjukov, V., Klyikov, D., Podbereznyi, V. and Shipilov, V. 1992. Floating nuclear desalination plant AFWS-40. Desalination. 89: 21–32.
Yang, W., Tian, W., Hvalbye, O., Peng, Z., Wei, K. and Tian, X. 2019. Experimental Research for Stabilizing Offshore Floating Wind Turbines. Energies. 12: 1947 (doi:10.3390/en12101947).
Zhang, Y., Zhao, J., Grabrick, B., Jacobson, B., Nelson, A. and Otte, J. 2018. Dynamic response of three floaters supporting vertical axis wind turbines due to wind excitation. Journal of Fluids and Structures. 80: 316-331.
Binrong Wen, Xinliang Tian, Xingjian Dong, Zhanwei Li, Zhike Peng, Wenming Zhang and Kexiang Wei. Design approaches of performance-scaled rotor for wave basin model tests of floating wind turbines. Renewable Energy, 148, 2020, pp 573-584.
Binrong Wen, Zhanwei Li, Zhihao Jiang, Xinliang Tian, Xingjian Dong and Zhike Peng. Blade loading performance of a floating wind turbine in wave basin model tests. Ocean Engineering, 199, 2020, pp 107061.